

Human Non-Hematopoietic CD271^{pos}/CD140a^{low/neg} Bone Marrow Stroma Cells Fulfill Stringent Stem Cell Criteria in Serial Transplantations

Roshanak Ghazanfari,^{1,2} Hongzhe Li,^{1,2} Dimitra Zacharaki,^{1,2} Hooi Ching Lim,^{1,2} and Stefan Scheduling¹⁻³

Human bone marrow contains a population of non-hematopoietic stromal stem/progenitor cells (BMSCs), which play a central role for bone marrow stroma and the hematopoietic microenvironment. However, the precise characteristics and potential stem cell properties of defined BMSC populations have not yet been thoroughly investigated. Using standard adherent colony-forming unit fibroblast (CFU-F) assays, we have previously shown that BMSCs were highly enriched in the nonhematopoietic CD271^{pos}/CD140a^{low/neg} fraction of normal adult human bone marrow. In this study, we demonstrate that prospectively isolated CD271^{pos}/CD140a^{low/neg} BMSCs expressed high levels of hematopoiesis supporting genes and signature mesenchymal and multipotency genes on a single cell basis. Furthermore, CD271^{pos}/CD140a^{low/neg} BMSCs gave rise to non-adherent sphere colonies (mesenspheres) with typical surface marker profile and trilineage in vitro differentiation potential. Importantly, serial transplantations of CD271^{pos}/CD140a^{low/neg} BMSC-derived mesenspheres (single cell and bulk) into immunodeficient NOD scid gamma (NSG) mice showed increased mesensphere numbers and full differentiation potential after both primary and secondary transplantations. In contrast, BMSC self-renewal potential decreased under standard adherent culture conditions. These data therefore indicate that CD271^{pos}/CD140a^{low/neg} BMSCs represent a population of primary stem cells with MSC phenotype and sphere-forming capacity that fulfill stringent functional stem cell criteria in vivo in a serial transplantation setting.

Keywords: bone marrow stromal cells, stem cells, BMSC, mesenspheres, self-renewal, serial transplantation

Introduction

HUMAN BONE MARROW contains a population of non-hematopoietic stromal stem/progenitor cells (BMSCs), which are important components of the hematopoietic stem cell niche, give rise to the hematopoietic stroma upon transplantation, and possess in vivo multilineage differentiation capacities toward skeletal lineages [1–3]. Despite their key role in bone marrow physiology, little is known about BMSC stem cell characteristics, which is mainly due to the fact that primary BMSCs have thus far been elusive for a precise phenotypical definition. However, recent progress has led to the identification of suitable markers/marker combinations to effectively enrich BMSCs [1,2,4–6], and furthermore, recently-developed non-adherent mesensphere cultures allowed to assay and amplify potent hematopoiesis-supporting BMSCs while preserving their undifferentiated phenotype [7].

Using these tools, the current study therefore aimed to investigate key phenotypical and, importantly, functional

stem cell properties of prospectively isolated human BMSCs. Our results clearly demonstrate for the first time that non-hematopoietic CD271^{pos}/CD140a^{low/neg} cells are stromal stem cells with in vivo self-renewal and differentiation potential in a serial transplantation setting.

Materials and Methods

Bone marrow mononuclear cells

In total, bone marrow samples (60 mL) were aspirated from the iliac crest bone of consenting healthy adult donors ($n=41$, median age 25 years, and range 19–35). The study was approved by the local ethics committee. Bone marrow mononuclear cells (BM-MNCs) were isolated by density gradient centrifugation (Ficoll-Paque Premium; GE Healthcare Life Sciences) following incubation with RosetteSep Human Mesenchymal Stem Cell Enrichment Cocktail (StemCell Technologies) for lineage depletion (CD3, CD14, CD19, CD38, CD66b, and glycophorin A).

¹Lund Stem Cell Center, University of Lund, Lund, Sweden.

²Division of Molecular Hematology, Department of Laboratory Medicine, University of Lund, Lund, Sweden,

³Department of Hematology, Skåne University Hospital, Lund, Sweden.

Fluorescence-activated cell sorting

Lineage-depleted BM-MNCs were incubated in blocking buffer [DPBS w/o Ca^{2+} , Mg^{2+} , 3.3 mg/mL human normal immunoglobulin (Octapharma)] and 1% fetal bovine serum (Life Technologies), followed by staining with monoclonal antibodies against CD45, CD271, and CD140a (for detailed information on the antibodies used in this study, please see Supplementary Materials and Methods; Supplementary Data are available online at www.liebertpub.com/scd). Sorting gates were set according to the corresponding fluorescence-minus-one (FMO) controls. Cells were sorted on a fluorescence activated cell sorting (FACS) Aria II or a FACS Aria III cell sorter (BD Biosciences). Dead cells were excluded by 7-amino-actinomycin (7-AAD; Sigma) staining, and doublets were excluded by gating on FSC-H versus FSC-W and SSC-H versus SSC-W. A description of the flow cytometric analysis is provided in the Supplementary Materials and Methods.

Non-adherent mesosphere cultures

Sorted BM-MNCs were plated at low density ($<1,000$ cells/cm²) in ultralow adherence plates (Corning) in sphere growth medium as described before [8]. The medium composition is described in detail in the Supplementary Materials and Methods. To prevent cell aggregation, cultures were left untouched for 1 week. Thereafter, half-medium changes were performed twice weekly. Spheres were passaged following enzymatic digestion with 0.25% type I collagenase (StemCell Technologies) for 30 min at 37°C, followed by washing with PBS, and replating at clonal density.

Generation of adherent marrow stromal cells and colony-forming unit fibroblast assays

Sorted BM-MNCs were cultured in standard MSC culture medium [StemMACS MSC Expansion Medium (Miltenyi Biotec, Bergisch Gladbach) plus 1% antibiotic-antimycotic solution (Sigma)]. Medium was changed weekly and passaged as described [2]. Colony-forming unit fibroblast (CFU-F) assays were performed as before [2] and as described in the Supplementary Materials and Methods.

In vitro differentiation assays

Stromal cells derived from adherent and sphere cultures were differentiated toward the adipogenic, osteogenic, and chondrogenic lineages as described [2]. Briefly, for adipogenic differentiation, cells were cultured for 14 days in AdipoDiff medium (Miltenyi Biotec) and stained with Oil red O (Sigma)

following fixation. For osteogenic differentiation, cells were cultured in osteogenesis induction medium (see Supplementary Materials and Methods) for 21 days and calcium depositions were visualized by alizarin red staining (Sigma). Chondrogenic differentiation was induced by culturing cell pellets for 28 days in chondrogenesis-induction medium (see Supplementary Materials and Methods). Cryosections of fixed pellets were stained with goat anti-human aggrecan, and nuclei were stained with 4', 6-diamidino-2-phenylindole (DAPI; Life Technologies). Sections were analyzed with an Axiovert 200M fluorescence microscope equipped with an AxioCam HRm camera (both from Carl Zeiss).

In vivo transplantation

For primary in vivo transplantations, sorted $\text{lin}^{\text{neg}}/\text{CD45}^{\text{neg}}/\text{CD271}^{\text{pos}}/\text{CD140a}^{\text{low/neg}}$ cells were expanded under non-adherent and adherent conditions. Spheres and colonies, respectively, were generated both from bulk sorted cells (seeded at clonal densities) and from single sorted cells. After expansion, cells were harvested and loaded overnight on hydroxyapatite/tricalcium phosphate ceramic powder (HA/TCP; Triosite, Zimmer) and then implanted s.c. into 8-week-old NOD.Cg-Prkdcscid Il2rgtm1Wjl/SzJ (NSG) mice.

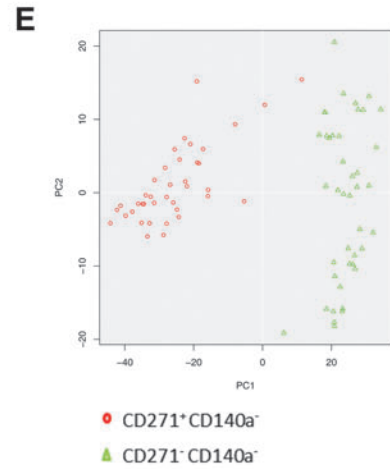
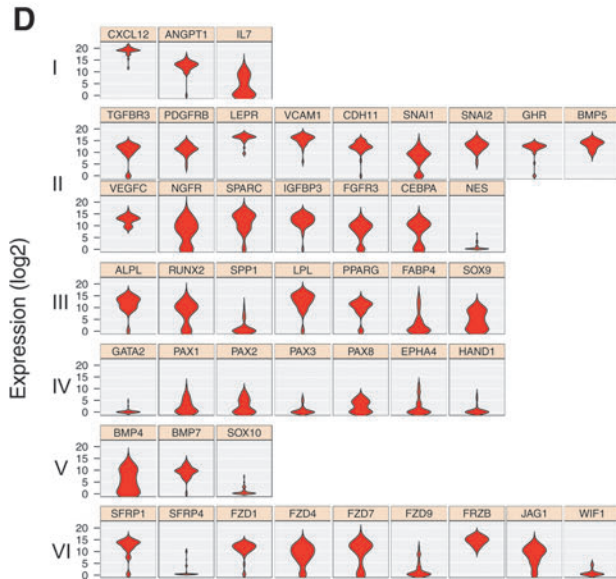
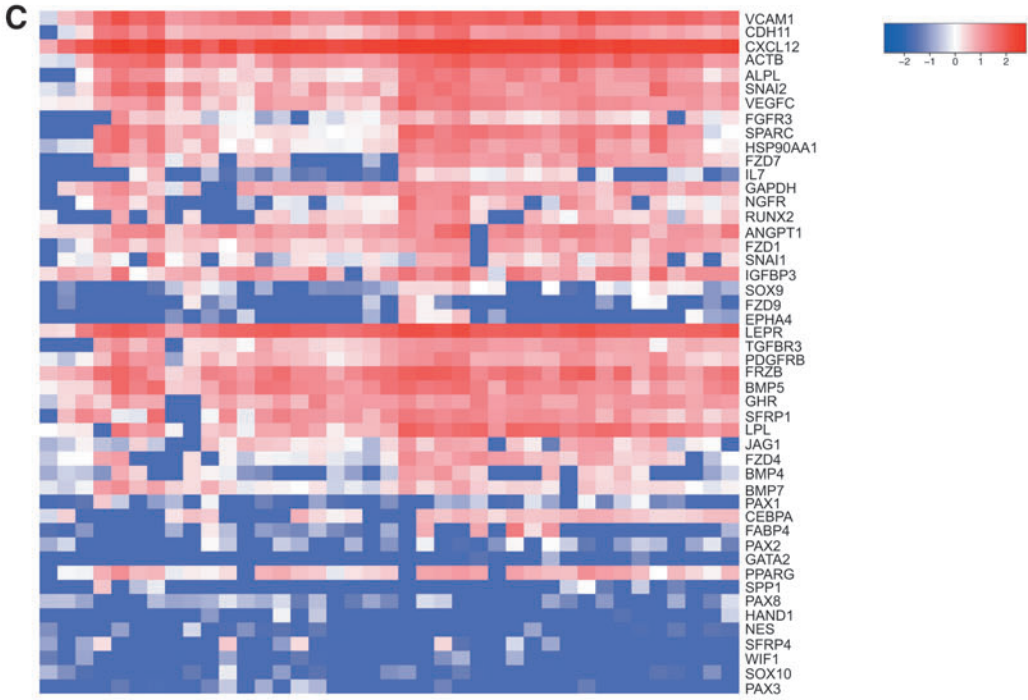
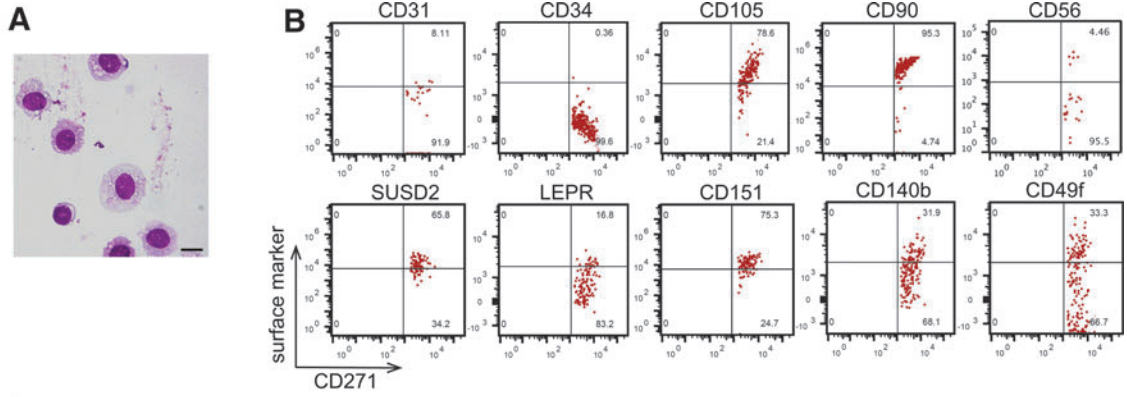
To evaluate in vivo self-renewal, implants were removed after 8 weeks, digested in 0.25% type I collagenase (STEMCELL Technologies) for 2 h at 37°C, and the harvested cells were stained with anti-mouse CD45 and anti-human CD90 and CD105 antibodies for FACS sorting. $\text{CD45}^{\text{neg}}/\text{CD90}^{\text{pos}}/\text{CD105}^{\text{pos}}$ sorted live cells (7AAD exclusion) were plated at clonal density for sphere and CFU-F colony formation. Spheres and CFU-Fs were enumerated after 10 and 14 days, respectively, and further expanded for secondary transplantations.

To assess the in vivo differentiation capacities, implants were removed after 8 weeks after primary and secondary sections were either stained with hematoxylin/eosin and analyzed as described [9] or prepared for immunohistochemistry as described below. The animal procedures were approved by the local ethics committee on animal experimentation.

Immunohistochemistry

Paraffin-embedded implanted samples were cut into 5 μm thick sections. Sections were deparaffinized and rehydrated following standard protocols [6]. Following antigen retrieval and blocking, sections were stained with primary antibodies (anti-vimentin, anti-mitochondria, and anti-CD45) and secondary antibodies followed by signal visualization (EnVision labeled polymer HRP; Dako) and microscopic examination using an

FIG. 1. Highly enriched $\text{CD271}^{\text{pos}}/\text{CD140a}^{\text{low/neg}}$ BMSCs display typical stromal cell characteristics. **(A)** Cytospin preparations of sorted human bone marrow (BM) $\text{CD271}^{\text{pos}}/\text{CD140a}^{\text{low/neg}}$ cells showed a typical primary BMSC morphology, that is, large immature nuclei with an open chromatin pattern and cytoplasmic vacuoles (May-Grunwald/Giemsa staining, scale bar represents 20 μm). **(B)** Flow cytometric surface marker co-expression analysis on primary $\text{CD271}^{\text{pos}}/\text{CD140a}^{\text{low/neg}}$ BMSCs. 2×10^6 events were acquired and plotted for CD271 versus the marker listed on the *top* after FSC/SSC gating, doublet, and dead cell exclusion (the gating strategy is illustrated in Supplementary Fig. S1A). A representative dataset is shown. **(C, D)** Single-cell gene expression analysis was performed on sorted $\text{CD271}^{\text{pos}}/\text{CD140a}^{\text{low/neg}}$ from three donors. The results are shown as heatmap, in which each of the 39 columns represents an individual cell **(C)** and as violin plots illustrating the expression level of the genes across the samples based on ANOVA **(D)**. Genes are listed according to function and cell type. Group I: hematopoietic supporting genes, group II: commonly expressed MSC genes, group III: differentiation-related genes, group IV: mesodermal markers, group V: neural crest markers, and group VI: signaling pathway genes. **(E)** Gene expression analysis of sorted single $\text{lin}^{\text{neg}}/\text{CD45}^{\text{neg}}/\text{CD271}^{\text{pos}}/\text{CD140a}^{\text{low/neg}}$ cells compared with non-CFU-F-containing $\text{lin}^{\text{neg}}/\text{CD45}^{\text{neg}}/\text{CD271}^{\text{neg}}/\text{CD140a}^{\text{neg}}$ cells from the same donors. The results are shown as Principal Component Analysis (PCA).



Olympus camera (BX51) and the cellSens Dimension software (Olympus). Details of the staining procedure are provided in the Supplementary Materials and Methods.

Quantitative RT-PCR

RNA from sorted CD90^{pos}CD105^{pos}, CD90^{neg}CD105^{neg}, and mouse CD45^{pos} cells recovered from implants after primary transplantation was isolated from four individual donors. cDNA was synthesized, and quantitative real-time PCR analysis was performed (for more details, see Supplementary Materials and Methods).

Single-cell real-time PCR (Fluidigm)

Primary BM-MNCs were sorted based on the expression of CD271 and CD140a. Lin^{neg}/CD45^{neg}/CD271^{pos}/CD140a^{low/neg} and lin^{neg}/CD45^{neg}/CD271^{neg}/CD140a^{neg} single cells were sorted directly into lysis buffer containing low EDTA TE buffer (Teknova), NP-40 (Sigma), and SUPERaseIn (Life Technologies). cDNA synthesis of single cells was performed using the qScript cDNA SuperMix Kit (Quanta Bioscience). Specific Target Amplification of 48 genes of interest (genes are listed in Supplementary Table S1) was carried out using the TATAA PreAmp GrandMaster Mix Kit (TATAA Biocenter) and the final product underwent exonuclease treatment (Exonuclease I Kit; New England Biolabs). The samples were mixed with EvaGreen Supermix-low ROX (Bio-Rad) and DNA binding dye and loading reagent (both from Fluidigm), loaded onto the 48.48 Dynamic Array IFC chip, and run on the BioMark™ (Fluidigm) system. Data analysis was performed using the BioMark Real-Time PCR Analysis and Singular Analysis Toolset software (Fluidigm). The grouping of the genes as presented in the violin plot analysis was based on published information on gene functions.

Statistical analysis

Data are expressed as mean ± standard deviation (mean ± SD). Student's *t*-test and ANOVA were used for statistical analysis.

Results and Discussion

Phenotypical and sphere-forming properties of primary CD271^{pos}/CD140a^{low/neg} BMSCs

In the last years, considerable progress has been made in the identification of human primary BMSC markers [3,5]. We have previously reported that lin^{neg}/CD45^{neg}/CD271^{pos}/CD140a^{low/neg} human bone marrow cells (hereinafter referred to as CD271^{pos}/CD140a^{low/neg} cells) represented a (close to) pure population of stromal progenitor cells [6].

As reported, freshly-sorted CD271^{pos}/CD140a^{low/neg} cells showed typical morphological BMSC features (Fig. 1A) [2,10] and expressed a typical "mesenchymal" stromal cell (MSC) surface marker profile (Fig. 1B) [5,6,11]. Expression of CD56, which was reported to identify bone-lining BMSCs [5], was limited to a small fraction of the cells (Fig. 1B). Thus, CD56 might be a possible positive marker for endosteal niche BMSCs, complementary to the negative expression of CD146 that we previously reported for this cell population [2]. Expression of integrin $\alpha 6$ (CD49f) on cultured MSC has been implicated in enhancing stem cell properties [12]. Interestingly, CD49f was clearly expressed in about one third of the

CD271^{pos}/CD140a^{low/neg} cells (Fig. 1B), which might indicate a possible role of CD49f in maintaining stemness of primary BMSCs. Certainly, this is an interesting point that will be addressed in future experiments.

Gene expression profiling of prospectively enriched BMSC has been reported for bulk sorted cells [6,13,14], which has obvious limitations when aiming to characterize highly-purified BMSCs. We therefore investigated the expression of a panel of selected BMSC-relevant genes in single-sorted CD271^{pos}/CD140a^{low/neg} cells (Fig. 1C, D and Supplementary Table S1).

CD271^{pos}/CD140a^{low/neg} cells showed a high and homogeneous expression of *CXCL12* and *ANGPT* (Fig. 1D, group I), the majority of common MSC-related genes (group II), most of the differentiation genes (group III), as well as Wnt signaling pathway-related genes (group VI), which are in accordance with published data on bulk sorted cells [13,14]. Interestingly, *IL-7* expression was heterogeneous (group I), which might point to a differential function of BMSC subsets in bone marrow lymphopoiesis. Furthermore, variances in expression of chondrocyte differentiation marker *SOX9* (Fig. 1D, group III) are likely to reflect differentiation potential differences. Low expression levels were observed for *NES* (group II), *SOX10* (group V), as well as several group IV and VI genes. Finally, CD271^{pos}/CD140a^{low/neg} cells clearly formed a distinct population as identified by principal component analysis compared with the non-CFU-F-containing CD271^{neg} cells (Fig. 1E).

In vitro, CD271^{pos}/CD140a^{low/neg} cells formed typical spheres (Fig. 2A) and CFU-F (not shown), the latter being the standard classical assay for clonogenic BM stromal cells. Progenitor cell frequencies of sorted CD271^{pos}/CD140a^{low/neg} BMSCs were comparable in both assays (Fig. 2B), and crossover replating experiments demonstrated that spheres and CFU-Fs had similar capacities to form secondary and tertiary CFU-Fs and spheres, respectively (Fig. 2C). Furthermore, CD271^{pos}/CD140a^{low/neg}-derived spheres exhibited a typical surface marker profile and in vitro differentiation pattern (Fig. 2D, E), and increasing sphere numbers in vitro were observed up to the second passage (Fig. 2F), which was comparable to standard CFU-F cultures (Fig. 2G).

Taken together, these data indicate that CD271^{pos}/CD140a^{low/neg} cells represent a highly enriched population of BMSCs with phenotypical stroma cell properties and in vitro mesosphere-forming capacity.

In vivo stem cell functions of CD271^{pos}/CD140a^{low/neg} BMSCs

Previous reports demonstrated in vitro stem/progenitor cell properties of human BMSCs [15,16]. However, true stem cell properties cannot be assessed in vitro, but only in vivo by proving that a putative stem cell can generate cells that are functionally equivalent to the original.

Evidence that primary BMSCs are stem cells comes from seminal studies demonstrating that single CFU-F-derived clonal cells were capable of generating bone and hematopoietic stroma in vivo and that secondary CFU-F could be recovered from the transplants [1]. Furthermore, in vivo self-renewal of clonogenic cells was demonstrated for fetal human and adult murine BMSCs using the mesosphere assay [8,17]. However, whether or not adult human BMSCs fulfill stringent stem cell criteria in a serial transplantation setting has not been thoroughly addressed thus far, although

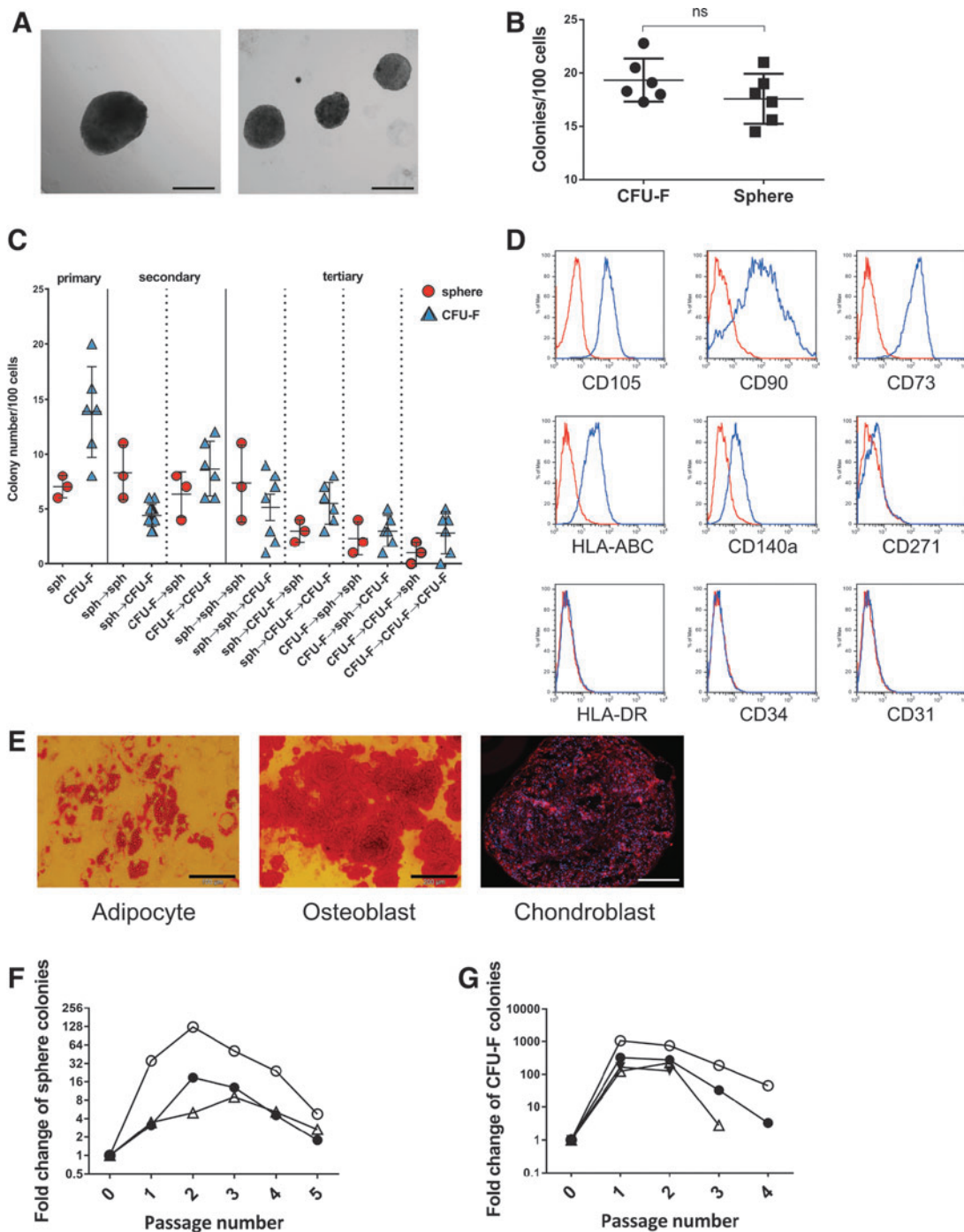


FIG. 2. In vitro potential of $\text{lin}^{\text{neg}}/\text{CD45}^{\text{neg}}/\text{CD271}^{\text{pos}}/\text{CD140a}^{\text{low/neg}}$ human bone marrow stromal cells. **(A)** $\text{CD271}^{\text{pos}}/\text{CD140a}^{\text{low/neg}}$ BMSCs were sorted and assayed as spheres. The morphology of typical spheres is shown in **(A)** (scale bar indicates 200 μm). **(B)** Frequencies of CFU-F and spheres in bulk-sorted $\text{lin}^{\text{neg}}/\text{CD45}^{\text{neg}}/\text{CD271}^{\text{pos}}/\text{CD140a}^{\text{low/neg}}$ cells were comparable (data are presented as mean \pm SD, $n=6$). **(C)** Sorted $\text{lin}^{\text{neg}}/\text{CD45}^{\text{neg}}/\text{CD271}^{\text{pos}}/\text{CD140a}^{\text{low/neg}}$ cells were assayed in standard adherent culture as CFU-F and as sphere colonies in sphere cultures. CFU-F and sphere colonies were then harvested and replated under both, CFU-F and sphere conditions, for two additional passages. Data are given for individual experiments with spheres and CFU-F indicated by *circles* (\circ) and *triangles* (Δ), respectively. *Arrows* used in the *x*-axis labels indicate switch to the next culture condition, for example, “sph \rightarrow CFU-F \rightarrow sph” indicates that cells initially cultured under sphere conditions were recultured as CFU-F, and finally cultured as tertiary colonies under sphere conditions. **(D)** Spheres showed a typical MSC surface marker profile; a representative set of data with passage 3 cells of a total of three experiments is shown. *Blue line*: spheres; *red line*: corresponding isotype control. **(E)** Trilineage in vitro differentiation potential of $\text{CD271}^{\text{pos}}/\text{CD140a}^{\text{low/neg}}$ BMSC-derived spheres. A representative set of pictures from a total of three experiments with passage 2 cells is shown; scale bars represent 100 μm (adipocyte) and 200 μm (osteoblast and chondrocyte). **(F)** $\text{CD271}^{\text{pos}}/\text{CD140a}^{\text{low/neg}}$ BMSC-derived spheres were harvested and replated up to four times. A net increase of sphere numbers was observed for the first and second passages, respectively. Data are presented as -fold change from three independent experiments indicated by different symbols. **(G)** $\text{CD271}^{\text{pos}}/\text{CD140a}^{\text{low/neg}}$ BMSC-derived CFU-Fs were harvested and replated up to four times. Data are presented as -fold change from four independent experiments indicated by different symbols. Sph, spheres.

this is an important aspect when characterizing the nature and function of primary native BMSCs.

We therefore short-term expanded single-cell and bulk-sorted CD271^{pos}/CD140a^{low/neg} BMSCs as spheres followed by subcutaneous implantation into immunodeficient mice (Fig. 3A). After 8 weeks, implants were harvested, assayed for human spheres, and then retransplanted into secondary recipients. FACS-isolation of human transplanted cells was performed based on the expression of human CD90 and CD105 (Supplementary Fig. S2A). CD90 and CD105 were chosen as sorting markers because of their relative stable expression in the transplanted cells in contrast to other markers. The sorting strategy and detection approach were validated by qPCR

analysis of human and mouse housekeeping genes (Supplementary Fig. S2B).

In vivo self-renewal of CD271^{pos}/CD140a^{low/neg} BMSCs was demonstrated by increasing number of spheres after primary and secondary transplantation compared with pre-transplantation values for both bulk-sorted (1.16 ± 0.06 and 2.34 ± 0.13-fold, respectively, n = 3) and single cell-derived spheres (1.54 ± 0.28 and 2.51 ± 0.72-fold, n = 3) (Fig. 3B and Supplementary Table S2). In contrast, implantation of adherently cultured CFU-Fs resulted in a more than 100-fold reduction of colony numbers after primary transplantation (Supplementary Fig. S2C), and therefore, secondary CFU-F transplantations were not performed.

In addition to in vivo sphere self-renewal, CD271^{pos}/CD140a^{low/neg} BMSCs demonstrated serial in vivo differentiation capacity. Transplanted spheres generated human bone, adipocytes, and stromal tissues after primary and secondary implantation, with murine hematopoietic cells invading the implants (Fig. 3C, D, respectively). There is cumulating evidence that differentiation potentials differ between stromal cells depending on their tissue of origin [18–20]. Our current work focused on BMSC and it therefore remains to be investigated whether or not stromal cell preparations from other sources have similar sphere formation and serial in vivo transplantation capacities.

Taken together, these results indicate that primary CD271^{pos}/CD140a^{low/neg} BMSCs are capable of in vivo self-renewal and differentiation. Cultures, which contained growth factors and prevented adherence to plastic, but not standard

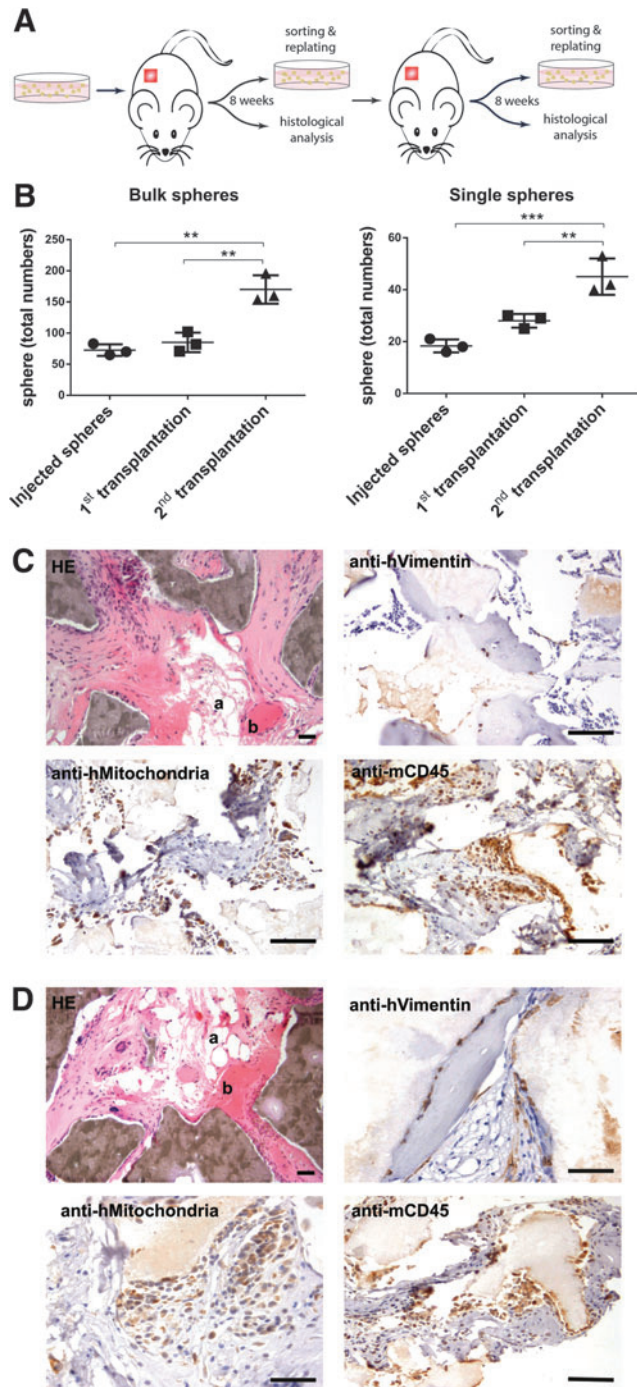


FIG. 3. In vivo self-renewal and differentiation capacity of lin^{neg}/CD45^{neg}/CD271^{pos}/CD140a^{low/neg} human bone marrow stromal cells. (A) Lin^{neg}/CD45^{neg}/CD271^{pos}/CD140a^{low/neg} cells were sorted (bulk and single cell) and tested for in vivo self-renewal and differentiation as depicted in the schematic drawing. CD271^{pos}/CD140a^{low/neg}-derived spheres (or CFU-Fs) were injected s.c. into NSG mice, explanted, sorted for human cells, analyzed, and retransplanted. Following another 8 weeks after secondary transplantation, cells were sorted again based on the expression of human-specific markers and analyzed (A). As shown in (B), bulk and single cell-derived spheres from sorted CD271^{pos}/CD140a^{low/neg} cells clearly demonstrated in vivo self-renewal indicated by increased numbers of total spheres after primary and secondary transplantations (data are given as mean ± SD, n = 3, **P < 0.01, and ***P < 0.001). In contrast, numbers of CD271^{pos}/CD140a^{low/neg}-derived CFU-F decreased after primary transplantation (Supplementary Fig. S2C). (C, D) Formation of ectopic tissues following primary and secondary transplantations of spheres derived from CD271^{pos}/CD140a^{low/neg} cells. Spheres were implanted subcutaneously with HA carrier into NSG mice. Representative sections 8 weeks after primary and secondary transplantation are shown in (C) and (D), respectively. The photomicrographs in the upper row left demonstrated generation of bone (b), adipocytes (a), and stromal tissues (Hematoxylin eosin staining, HE). Dark brown areas represent HA/TCP particles. Immunohistochemical staining with anti-human vimentin (upper row, right), anti-human mitochondria (lower row, left), and anti-mouse CD45 antibodies (lower row, right) indicates human and murine origin of the stromal tissues and hematopoietic cells, respectively. Scale bars represent 100 μm for HE and anti-CD45 staining, and 50 μm for anti-vimentin and anti-mitochondria staining. For controls, see Supplementary Figure S2D.

adherent cultures, enhanced stem cell properties and allowed to expand transplantable stromal stem cells, which is certainly an important finding for future studies aiming to design stroma stem cell replacement and repair strategies.

Acknowledgments

This work was supported by funds from the HematoLinné and Stem Therapy Program, the Swedish Cancer Foundation, the Swedish Childhood Cancer Foundation, Gunnar Nilsson's Cancer Foundation, Gunnel Björk's Testament, ALF (Government Public Health Grant), and the Skåne County Council's Research Foundation. The authors thank Helene Larsson and Anna Jonasson for help with the bone marrow samples, the Lund Stem Cell Center FACS facility for excellent technical assistance, and Dr. Simón Méndez-Ferrer (Wellcome Trust-Medical Research Council Cambridge Stem Cell Institute and NHS Blood and Transplant, Cambridge, United Kingdom) for critical discussions.

Author Disclosure Statement

The authors have no conflicts of interest to disclose.

References

- Sacchetti B, A Funari, S Michienzi, S Di Cesare, S Piersanti, I Saggio, E Tagliafico, S Ferrari, PG Robey, M Riminucci and P Bianco. (2007). Self-renewing osteoprogenitors in bone marrow sinusoids can organize a hematopoietic microenvironment. *Cell* 131:324–336.
- Tormin A, O Li, JC Brune, S Walsh, B Schutz, M Ehinger, N Ditzel, M Kassem and S Scheduling. (2011). CD146 expression on primary nonhematopoietic bone marrow stem cells is correlated with in situ localization. *Blood* 117:5067–5077.
- Keating A. (2012). Mesenchymal stromal cells: new directions. *Cell Stem Cell* 10:709–716.
- Jones EA, SE Kinsey, A English, RA Jones, L Straszynski, DM Meredith, AF Markham, A Jack, P Emery and D McGonagle. (2002). Isolation and characterization of bone marrow multipotential mesenchymal progenitor cells. *Arthritis Rheum* 46:3349–3360.
- Sivasubramanian K, D Lehnen, R Ghazanfari, M Sobiesiak, A Harichandan, E Mortha, N Petkova, S Grimm, F Cerabona, et al. (2012). Phenotypic and functional heterogeneity of human bone marrow- and amnion-derived MSC subsets. *Ann N Y Acad Sci* 1266:94–106.
- Li H, R Ghazanfari, D Zacharaki, N Ditzel, J Isern, M Ekblom, S Mendez-Ferrer, M Kassem and S Scheduling. (2014). Low/negative Expression of PDGFR-alpha identifies the candidate mesenchymal stromal cells in adult human bone marrow. *Stem Cell Rep* 3:965–974.
- Isern J, B Martín-Antonio, R Ghazanfari, AM Martín, R del Toro, A Sánchez-Aguilera, L Arranz, D Martín-Pérez, JA López, et al. (2013). Self-renewing human bone marrow mesospheres promote hematopoietic stem cell expansion. *Cell Rep* 3:1714–1724.
- Mendez-Ferrer S, TV Michurina, F Ferraro, AR Mazloom, BD Macarthur, SA Lira, DT Scadden, A Ma'ayan, GN Enikolopov and PS Frenette. (2010). Mesenchymal and haematopoietic stem cells form a unique bone marrow niche. *Nature* 466:829–834.
- Abdallah BM, N Ditzel and M Kassem. (2008). Assessment of bone formation capacity using in vivo transplantation assays: procedure and tissue analysis. *Methods Mol Biol* 455:89–100.
- Buhring HJ, VL Battula, S Treml, B Schewe, L Kanz and W Vogel. (2007). Novel markers for the prospective isolation of human MSC. *Ann N Y Acad Sci* 1106:262–271.
- Sivasubramanian K, A Harichandan, S Schumann, M Sobiesiak, C Lengerke, A Maurer, H Kalbacher and HJ Buhring. (2013). Prospective isolation of mesenchymal stem cells from human bone marrow using novel antibodies directed against Sushi domain containing 2. *Stem Cells Dev* 22:1944–1954.
- Yu KR, SR Yang, JW Jung, H Kim, K Ko, DW Han, SB Park, SW Choi, SK Kang, H Scholer and KS Kang. (2012). CD49f enhances multipotency and maintains stemness through the direct regulation of OCT4 and SOX2. *Stem Cells* 30:876–887.
- Churchman SM, F Ponchel, SA Boxall, R Cuthbert, D Kouroupis, T Roshdy, PV Giannoudis, P Emery, D McGonagle and EA Jones. (2012). Transcriptional profile of native CD271+ multipotential stromal cells: evidence for multiple fates, with prominent osteogenic and Wnt pathway signaling activity. *Arthritis Rheum* 64:2632–2643.
- Qian H, K Le Blanc and M Sigvardsson. (2012). Primary mesenchymal stem and progenitor cells from bone marrow lack expression of CD44 protein. *J Biol Chem* 287:25795–25807.
- Muraglia A, R Cancedda and R Quarto. (2000). Clonal mesenchymal progenitors from human bone marrow differentiate in vitro according to a hierarchical model. *J Cell Sci* 113(Pt 7):1161–1166.
- Lee CC, JE Christensen, MC Yoder and AF Tarantal. (2010). Clonal analysis and hierarchy of human bone marrow mesenchymal stem and progenitor cells. *Exp Hematol* 38:46–54.
- Pinho S, J Lacombe, M Hanoun, T Mizoguchi, I Bruns, Y Kunisaki and PS Frenette. (2013). PDGFRalpha and CD51 mark human nestin+ sphere-forming mesenchymal stem cells capable of hematopoietic progenitor cell expansion. *J Exp Med* 210:1351–1367.
- Rolandsson S, AA Sjolund, JC Brune, H Li, M Kassem, F Mertens, A Westergren, L Eriksson, L Hansson, et al. (2014). Primary mesenchymal stem cells in human transplanted lungs are CD90/CD105 perivascularly located tissue-resident cells. *BMJ Open Respir Res* 1:e000027.
- Reinisch A, N Etchart, D Thomas, NA Hofmann, M Fruehwirth, S Sinha, CK Chan, K Senarath-Yapa, EY Seo, et al. (2015). Epigenetic and in vivo comparison of diverse MSC sources reveals an endochondral signature for human hematopoietic niche formation. *Blood* 125:249–260.
- Sacchetti B, A Funari, C Remoli, G Giannicola, G Kogler, S Liedtke, G Cossu, M Serafini, M Sampaolesi, et al. (2016). No identical “Mesenchymal Stem Cells” at different times and sites: human committed progenitors of distinct origin and differentiation potential are incorporated as adventitial cells in microvessels. *Stem Cell Rep* 6:897–913.

Address correspondence to:

Stefan Scheduling, MD
Division of Molecular Hematology
Department of Laboratory Medicine
University of Lund
BMC B12, Klinikgatan 26
Lund 22184
Sweden

E-mail: stefan.scheduling@med.lu.se

Received for publication June 10, 2016
 Accepted after revision August 12, 2016

Prepublished on Liebert Instant Online August 12, 2016